Generation of low-frequency electrostatic and electromagnetic waves as nonlinear consequences of beam–plasma interactions

Takayuki Umeda[a)]
Solar-Terrestrial Environment Laboratory, Nagoya University, Nagoya, Aichi 464-8601, Japan

(Received 20 February 2008; accepted 9 May 2008; published online 25 June 2008)

Nonlinear evolution of the electron two-stream instability in a current-carrying plasma is examined by using a two-dimensional electromagnetic particle-in-cell simulation. Formation of electron phase-space holes is observed as an early nonlinear consequence of electron–beam–plasma interactions. Lower-hybrid waves, electrostatic, and electromagnetic whistler mode waves are also excited by different mechanisms during the ensuing nonlinear wave–particle interactions. It is shown by the present computer simulation with a large simulation domain and a long simulation time that these low-frequency waves can disturb the electrostatic equilibrium of electron phase-space holes, suggesting that the lifetime of electron phase-space holes sometimes becomes shorter in a current-carrying plasma. © *2008 American Institute of Physics*.
[DOI: 10.1063/1.2937818]

It is well-known from early computer simulations of the Vlasov–Poisson system in the 1960s that coherent electrostatic potential structures are generated as a consequence of nonlinear beam–plasma interactions.[1,2] These coherent structures consist of charged particles trapped by an electrostatic potential well of the coherent structure, and appear as rotating vortices around holes in the position-velocity phase space. These structures were also observed in laboratory plasmas.[3] The phase-space structures of these holes have been modeled by using one-dimensional equilibrium solutions to the time-independent Vlasov–Poisson equations called the Bernstein–Greene–Kruskal (BGK) equilibrium (e.g., Refs. 4–6).

The electron phase-space holes have been invoked to interpret electrostatic solitary waves (ESWs) observed in the geomagnetospheric plasma during broadband electrostatic noise (BEN) events.[7] The ESWs are bipolar electric pluses without a magnetic component, whose polarization is longitudinal to the ambient magnetic field turning from positive to negative or from negative to positive in a few milliseconds.[8] It has been demonstrated by computer simulation studies that there is a close similarity between characteristics of observed ESWs and electron phase-space holes generated by nonlinear electron–beam–plasma interactions.[9] The ESWs are likely to be one part of the BEN emissions, because such electric pulses have a broad range of frequencies below the electron plasma frequency. The electrostatic solitary structures are commonly observed in the auroral region[10] and other boundary layers[11] of planetary magnetospheres. Thus beam–plasma interactions are one of the ubiquitous processes in space plasmas.

Recent computer simulations have demonstrated that electron–beam–plasma interactions show highly complex features in multidimensions. Electron phase-space holes or BGK modes, which are stable in one-dimensional systems, are sometimes unstable in multidimensional systems. The phase-space holes quickly dissipate in a weakly magnetized plasma,[2,12,13] whereas a stronger magnetic field enables electron holes to persist for a longer time.[6,13–15] Electrostatic whistler mode waves are excited as a nonlinear consequence of electron–hole–plasma interaction in a strongly magnetized plasma.[13,16] However, the electrostatic whistler waves are not excited when the potential energy of an individual electron hole $e\phi$ is much smaller than the effective thermal energy of surrounding background electrons after the saturation of beam instability,[13,14] where ϕ is the peak-to-bottom value of electrostatic potential. Instead, lower-hybrid waves are excited by an interaction between electron holes and ions.[14,15]

The coherent structures seen in satellite observations and in computer simulations of beam–plasma interactions were electrostatic with very weak or without magnetic component.[8,10,18] Thus interests in previous studies were limited to electrostatic problems in which only Poisson's equation is solved. In this paper, generation of electromagnetic waves and ensuring nonlinear processes of electron–beam–plasma interactions are of interest. We performed a computer simulation using an electromagnetic particle-in-cell code with two spatial and three velocity dimensions.[19] A full set of Maxwell's equations and the equations of motion for individual charged particles are solved in a self-consistent manner with the standard leapfrog algorithms,[20] while the current density is computed with the charge conservation method.[21]

The simulation domain is taken in the $x-y$ plane with $N_x \times N_y = 4096 \times 512$ grid points. The ambient magnetic field is taken in the x direction. In both x and y directions we imposed periodic boundary conditions for both fields and particles. We assumed counterstreaming two electron beams with an equal density $0.5n_e$ and equal initial thermal velocity V_{te}. The two electron beams drift along the ambient magnetic field with the drift velocities V_d and $-V_d$. Ions with an initial thermal velocity V_{ti} and a density $n_i = n_e$ are also assumed to be drifting along the ambient magnetic field with the drift velocity $-V_d$.

Assuming the total electron plasma frequency $\omega_{pe} = 1.0$

a)Electronic mail: umeda@stelab.nagoya-u.ac.jp.

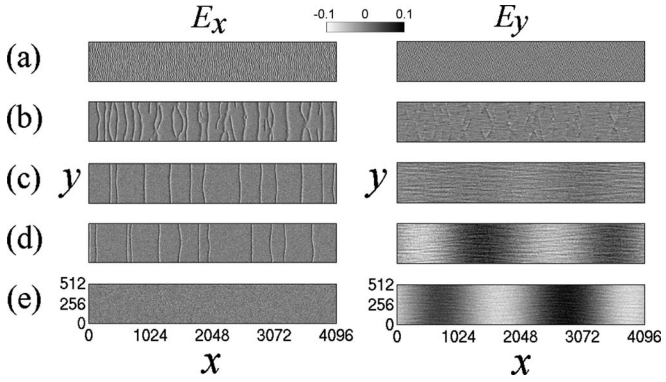

FIG. 1. Spatial profiles of the electric field E_x and E_y at different times. (a) $\omega_{pe}t=50$, (b) $\omega_{pe}t=1000$, (c) $\omega_{pe}t=4000$, (d) $\omega_{pe}t=6000$, and (e) $\omega_{pe}t=8000$. The amplitude is normalized by $m_e\omega_{pe}V_d/e$, and the distance is normalized by V_{te}/ω_{pe}.

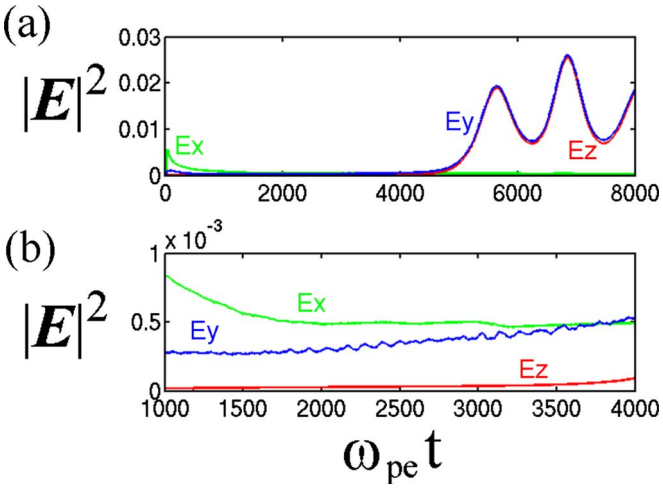

FIG. 2. (Color online) (a) Time history of the electric field energies $|E_x|^2$, $|E_y|^2$, and $|E_z|^2$ normalized by $m_e^2\omega_{pe}^2V_d^2/e^2$. (b) Expanded history for $\omega_{pe}t=1000-4000$.

and the initial electron thermal velocity $V_{te}=1.0$, we normalize the frequency and velocity by ω_e and V_{te}, respectively. The distance is normalized by the initial electron Debye length $\lambda_e=V_{te}/\omega_{pe}$. The drift velocity is set to be $V_d/V_{te}=2.0$, and the electron cyclotron frequency is set to be $\omega_{ce}/\omega_{pe}=4.0$. Here we use the real ion-to-electron mass ratio $m_i/m_e=1836$ with the temperature ratio $T_i/T_e=4.0$. To increase computation efficiency, however, we assumed a reduced light speed $c=10.0V_{te}$. The grid spacings Δx and Δy are equal to $1.0V_{te}/\omega_{pe}$, and the time step is equal to $\omega_{pe}\Delta t=0.05$. We used 256 particles per cell for each species. Thus over 1600 million particles are totally employed.

In a previous study of the electron two-stream instability *without* ion dynamics, a stable one-dimensional electron hole was formed at the final phase of nonlinear evolution with these parameters.[13] In contrast, we include ion dynamics in the present study, and ion modes are likely excited. Thus we take a large simulation domain and a long simulation time. In the present study, the simulation domain is taken in the rest frame of electron phase-space holes, while ions drift against the phase-space holes in the $-x$ direction. Thus there exists a current in this simulation model. Note that this model was adopted in previous simulations[14,16] and in the present one because the ion dynamics leads to the disruption of electron phase-space holes when the relative velocity between ions and phase-space holes is slower than the ion-acoustic speed.[9,22]

It is also noted that the effective temperature of electrons after the saturation of beam instability is $T_{\mathrm{ef}}\sim 4T_e$. Since the temperature ratio between ions and electrons after the saturation of beam instability becomes about $T_{\mathrm{ef}}/T_i\sim 1$, there is no excitation of ion acoustic waves. The maximum velocity of electrons after the saturation of beam instability also becomes $v_{\max}\sim 6V_{te}$. Thus we assume a nonrelativistic regime.

Figure 1 shows spatial profiles of the electric field E_x and E_y at different times. In the two-dimensional system consisting of spatial coordinates parallel and perpendicular to the ambient magnetic field, there exists seed fluctuations with finite wave numbers $k_\parallel$ and $k_\perp$. The parallel electron beam mode ($k_\perp=0$) as well as the oblique electrostatic modes ($k_\perp\neq 0$) grow linearly as the time elapses. At the saturation phase of the instability ($\omega_{pe}t\sim 50$), there exists two-dimensional sinusoidal potential structures [Fig. 1(a)]. In the subsequent nonlinear evolution, the two-dimensional potentials coalesce with each other, forming isolated potential humps, i.e., electron phase-space holes. The electron phase-space holes have bipolar structures in the electric field parallel to the ambient magnetic field as seen in Fig. 1(b). During the coalescence of electron phase-space holes, they are aligned in the direction perpendicular to the ambient magnetic field with the perpendicular electric field diminishing slowly. The two-dimensional characteristics totally disappear from the potential structures, and one-dimensional potential structures appear [Fig. 1(c)], which are essentially BGK modes. These are typical processes of the evolution of electron holes in the multidimensional system.

Figure 2 shows time history of the electric field energies $|E_x|^2$, $|E_y|^2$, and $|E_z|^2$ normalized by $m_e^2\omega_{pe}^2V_d^2/e^2$. The parallel electric field E_x saturates at a very early phase ($\omega_{pe}t\sim 50$), corresponding to the saturation of the electron beam instability. After the saturation of the parallel electric field E_x, the perpendicular electric field E_y grows slowly from $\omega_{pe}t\sim 1500$ [see the expanded history for $\omega_{pe}t=1000-4000$ in Fig. 2(b)], which corresponds to the generation of low-frequency electrostatic mode. The frequency of this mode is roughly estimated to be $\omega\sim 0.06\omega_{pe}$. The low-frequency electrostatic mode have a long wavelength in the direction parallel to the ambient magnetic field and a short wavelength in the direction perpendicular to the ambient magnetic field as seen in Fig. 1(c).

From $\omega_{pe}t\sim 3500$ both E_y and E_z components show increase in the electric field energy, corresponding to the excitation of an electromagnetic wave because the E_z component consists only of the electromagnetic field while the E_y component consists of both electrostatic and electromagnetic fields in the two-dimensional system taken in the $x-y$ plane. The amplitude of the electromagnetic wave becomes much higher than that of the saturation level of the parallel electric field E_x. The frequency of the electromagnetic wave is estimated as $\omega\sim 0.008\omega_{pe}$, which is lower than the lower hybrid

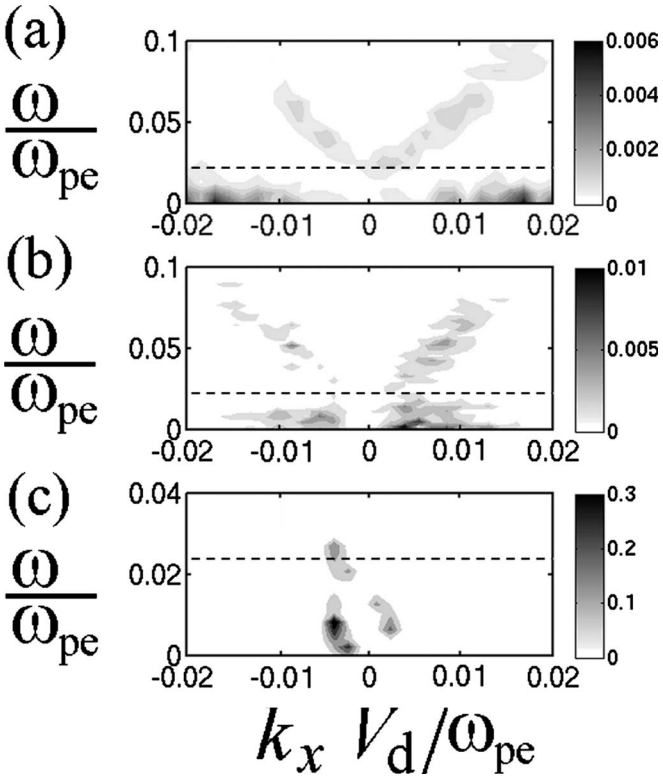

FIG. 3. Parallel-wavenumber-frequency spectra of a perpendicular electric field component E_y at different time intervals. (a) $\omega_{pe}t=0-1000$, (b) $\omega_{pe}t=2000-4000$, and (c) $\omega_{pe}t=6000-8000$. The amplitude is normalized by $m_e\omega_{pe}V_d/e$. Note that these spectra show projection of $|E_y(\omega,k_x,k_y)|$ on to $k_y=0$. The dashed line indicates the lower hybrid resonance frequency. Note that a more intense gray scale is used for a later time interval.

resonance frequency ($\omega_{\mathrm{LHR}}=0.0233\omega_{pe}$) but is higher than the ion cyclotron frequency ($\omega_{ci}=0.0022\omega_{pe}$). The electromagnetic wave has a long wavelength in the direction parallel to the ambient magnetic field but does not have any structure in the direction perpendicular to the ambient magnetic field as seen in Fig. 1(d).

Figure 3 shows parallel-wavenumber-frequency spectra (i.e., numerical dispersion relation) of the E_y component at different time intervals. Note that these spectra show projection of $|E_y(\omega,k_x,k_y)|$ on to $k_y=0$. For $\omega_{pe}t=0\sim1000$, the spectrum of the E_y component shows a weak enhancement at low-frequencies by linearly unstable wave modes propagating obliquely to the ambient magnetic field. For $\omega_{pe}t=2000-4000$, the spectrum of the E_y component shows a strong enhancement at a very low frequency $\omega\sim0.004\omega_{pe}$ and in a wide frequency range ($\omega/\omega_{pe}=0.03-0.08$). The higher-frequency component is an electrostatic whistler mode whose frequency is higher than the lower-hybrid resonance frequency but is much lower than the electron cyclotron frequency *in the rest frame of electrons*. It is also known that the phase velocity of electrostatic whistler mode waves is much faster than the initial electron beam speed,[13,17] which is consistent with the numerical dispersion relation in Fig. 3(b).

Umeda *et al.*[13] performed a two-dimensional simulation with the same simulation parameters as the present simulation but with a smaller simulation domain. However, electrostatic whistler mode waves were not excited in their simulation. Excitation of electrostatic whistler mode waves from electron phase-space holes likely takes place when the potential energy of electron phase-space holes becomes higher than the thermal energy of background electrons.[13] Since the simulation domain in the present simulation is much more elongated in the parallel direction than in the previous simulation, there exist more electron phase-space vortices, i.e., energy sources, at the saturation phase of the instability. Thus the potential energy of the large electron holes resulting from the coalescence of all the small holes can exceed the thermal energy of background electrons in the present simulation.

Although enhancement of the lower-frequency component is not apparent in Fig. 2(b), its existence has been clearly shown by the $\omega-k_x$ spectrum in Fig. 3(b). The phase velocity of this lower-frequency component is estimated as $v_p\sim0.5V_{te}$. Since ions are drifting in the negative $(-x)$ direction in the present simulation model, the Doppler effect in frequency should be taken into account. The frequency of this mode *in the rest frame of ions* is roughly estimated as $\omega/\omega_{pe}\sim0.004(v_p+V_d)/v_p\sim0.02$ which is close to the lower-hybrid resonance frequency. Thus we expect that the lower-frequency component in Fig. 3(b) is a lower-hybrid wave due to ion dynamics. Note that the phase velocity of lower-hybrid waves is almost equal to the propagation velocity of the electron phase-space holes in the rest frame of ions.[14,15]

For $\omega_{pe}t=6000-8000$, the spectrum of E_y shows a strong enhancement of an electromagnetic wave at a frequency $\omega\sim0.008\omega_{pe}$ and at a wavenumber $k_xV_{te}/\omega_{pe}\sim0.003$. The numerical dispersion relation shows that the electromagnetic wave propagates in the negative $(-x)$ direction at a phase velocity $v_p\sim-2.7V_{te}$, which is faster than the Alfvén speed ($V_A\sim0.9V_{te}$). Since an ion beam is propagating in the $-x$ direction at a velocity $V_d=-2V_{te}$, the anomalous ion cyclotron resonance condition, $\omega+\omega_{ci}=-V_dk_{\|}$, is almost satisfied. Thus we expect that an R-mode electromagnetic ion cyclotron (EMIC) wave is excited by a current-driven instability due to the drifting ion beam. It is noted that the EMIC wave is also excited even when the simulation is started with a warm electron beam of temperature T_{ef} without electron holes and an ion beam drifting at $-V_d$.

The particle-in-cell simulation presented here has shown that linearly unstable wave modes in a beam–plasma instability do not persist for a long time, diminishing during the coalescence of electron phase-space holes. Low-frequency electrostatic and electromagnetic waves are excited in the ensuing nonlinear processes. At the final phase of the simulation run [Fig. 1(e)], low-frequency electrostatic and electromagnetic waves persist, while electron phase-space holes disappear, implying the low-frequency (ion-scale) electrostatic and electromagnetic waves strongly affect the stability of electron holes. It is suggested by the present computer simulation with a large simulation domain and a long simulation time that the lifetime of electron phase-space holes in a current-carrying plasma becomes shorter when the relative velocity between background electrons and ions is faster than the Alfvén speed. Thus the electron holes are stable when the propagation speed of electron holes V_{EH} is faster

than the ion sound speed but is slower than the Alfvén speed, i.e., $C_s = V_{te}\sqrt{T_{\mathrm{ef}}/T_e}\sqrt{m_e/m_i} < V_{\mathrm{EH}} < V_A = c(\omega_{ce}/\omega_{pe})\sqrt{m_e/m_i}$. In the present study, the reduced speed of light artificially makes the Alfvén speed slower and causes the anomalous ion cyclotron resonance in a strongly magnetized plasma. In a weakly magnetized plasma, however, it is likely that the drift velocity of an ion beam is sometimes faster than the Alfvén speed even with a realistic speed of light, and the lifetime of electron holes becomes shorter in such cases.

The author is grateful to Y. Omura and H. Matsumoto for discussions. The computer simulation was performed on the AKDK supercomputer system at RISH in Kyoto University as a collaborative research project.

This work was in part supported by the Grant-in-Aid for Creative Scientific Research No. 17GS0208 from MEXT of Japan.

[1] K. V. Roberts and H. L. Berk, Phys. Rev. Lett. **19**, 297 (1967).
[2] R. L. Morse and C. W. Nielson, Phys. Rev. Lett. **23**, 1087 (1969).
[3] K. Saeki, P. Michelsen, H. L. Pecseli, and J. J. Rasmussen, Phys. Rev. Lett. **42**, 501 (1979).
[4] I. B. Bernstein, J. M. Greene, and M. D. Kruskal, Phys. Rev. **108**, 546 (1957).
[5] V. A. Turikov, Phys. Scr. **30**, 73 (1984); V. L. Krasovsky, H. Matsumoto, and Y. Omura, J. Geophys. Res. **102**, DOI: 10.1029/97JA02033 22131 (1997); **108**, DOI: 10.1029/2001JA000277 1117 (2003); L.-J. Chen, D. J. Thouless, and J.-M. Tang, Phys. Rev. E **69**, 055401(R) (2004).
[6] L. Muschietti, R. E. Ergun, I. Roth, and C. W. Carlson, Geophys. Res. Lett. **26**, 1093, DOI: 10.1029/1999GL900207 (1999).
[7] F. Scarf, L. A. Frank, K. Ackerson, and R. P. Lepping, Geophys. Res. Lett. **1**, 189, DOI: 10.1029/GL001i005p00189 (1974); D. A. Gurnett, L. A. Frank, and D. Lepping, J. Geophys. Res. **81**, 6059, DOI: 10.1029/JA081i034p06059 (1976).
[8] H. Matsumoto, H. Kojima, T. Miyatake, Y. Omura, M. Okada, I. Nagano, and M. Tsutsui, Geophys. Res. Lett. **21**, 2915, DOI: 10.1029/94GL01284 (1994); H. Matsumoto, L. A. Frank, Y. Omura, H. Kojima, W. R. Paterson, M. Tsutsui, R. R. Anderson, S. Horiyama, S. Kokubun, and T. Yamamoto, Geophys. Res. Lett. **26**, 421, DOI: 10.1029/1999GL900005 (1999); H. Kojima, H. Matsumoto, T. Miyatake, I. Nagano, A. Fujita, L. A. Frank, T. Mukai, W. R. Paterson, and R. R. Anderson, Geophys. Res. Lett. **21**, 2919, DOI: 10.1029/94GL02111 (1994).
[9] Y. Omura, H. Kojima, and H. Matsumoto, Geophys. Res. Lett. **21**, 2923, DOI: 10.1029/94GL01605 (1994); Y. Omura, H. Matsumoto, T. Miyake, and H. Kojima, J. Geophys. Res. **101**, 2685, DOI: 10.1029/95JA03145 (1996).
[10] F. S. Mozer, R. Ergun, M. Temerin, C. Cattell, J. Dombeck, and J. Wygant, Phys. Rev. Lett. **79**, 1281 (1997); R. E. Ergun, C. W. Carlson, J. P. McFadden, F. S. Mozer, L. Muschietti, I. Roth, and R. Strangway, *ibid.* **81**, 826 (1998).
[11] J. S. Pickett, L.-J. Chen, S. W. Kahler, O. Santolik, D. A. Gurnett, B. T. Tsurutani, and A. Balogh, Ann. Geophys. **22**, 2515 (2004).
[12] L. Muschietti, I. Roth, C. W. Carlson, and R. E. Ergun, Phys. Rev. Lett. **85**, 94 (2000).
[13] T. Umeda, Y. Omura, T. Miyake, H. Matsumoto, and M. Ashour-Abdalla, J. Geophys. Res. **111**, A10206, DOI: 10.1029/2006JA011762 (2006).
[14] T. Miyake, Y. Omura, and H. Matsumoto, J. Geophys. Res. **105**, 23239, DOI: 10.1029/2000JA000001 (2000).
[15] N. Singh, S. M. Loo, and B. E. Wells, J. Geophys. Res. **106**, 21183, DOI: 10.1029/2001JA900056 (2001); T. Umeda, Y. Omura, H. Matsumoto, and H. Usui, *ibid.* **107**, 1449, DOI: 10.1029/2001JA000286 (2002).
[16] M. V. Goldman, M. M. Oppenheim, and D. L. Newman, Geophys. Res. Lett. **26**, 1821, DOI: 10.1029/1999GL900435 (1999); M. M. Oppenheim, D. L. Newman, and M. V. Goldman, Phys. Rev. Lett. **83**, 2344 (1999); M. M. Oppenheim, G. Vetoulis, D. L. Newman, and M. V. Goldman, Geophys. Res. Lett. **28**, 1891, DOI: 10.1029/2000GL012383 (2001); F. J. Crary, M. V. Goldman, R. E. Ergun, and D. L. Newman, *ibid.* **28**, 3059, DOI: 10.1029/2001GL013050 (2001); D. L. Newman, M. V. Goldman, M. Spector, and F. Perez, Phys. Rev. Lett. **86**, 1239 (2001); G. Vetoulis and M. Oppenheim, *ibid.* **86**, 1235 (2001).
[17] M. V. Goldman, F. Crary, D. L. Newman, and M. M. Oppenheim, Phys. Plasmas **7**, 1732 (2000).
[18] T. Umeda, Y. Omura, and H. Matsumoto, J. Geophys. Res. **109**, A02207, DOI: 10.1029/2003JA010000 (2004).
[19] T. Umeda, Ph.D. thesis, Kyoto University (2004).
[20] Y. Omura and H. Matsumoto, "KEMPO1: Technical guide to one-dimensional electromagnetic particle code," in *Computer Space Plasma Physics*, edited by H. Matsumoto and Y. Omura (Terra Scientific, Tokyo, 1993), pp. 21–65.
[21] T. Umeda, Y. Omura, T. Tominaga, and H. Matsumoto, Comput. Phys. Commun. **156**, 73 (2003).
[22] K. Saeki and H. Genma, Phys. Rev. Lett. **80**, 1224 (1998).